DRIFTS Evidence for Facet-Dependent Adsorption of Gaseous Toluene on TiO2 with Relative Photocatalytic Properties

DRIFTS Evidence for Facet Dependent Adsorption of Gaseous Toluene on TiO_2 with Relative Photocatalytic Properties

Mengjiao Wang [†], Fan Zhang [‡], Xiaodi Zhu [‡], Zeming Qi [‡], Bin Hong [‡], Jianjun Ding [†, ‡], Jun Bao [†, ‡], Song Sun [†, ‡], Chen Gao* [†, ‡]*

† CAS Key Laboratory of Materials for Energy Conversion, Department of Materials Science and Engineering, University of Science & Technology of China, Hefei, Anhui, 230026, China

‡ National Synchrotron Radiation Laboratory, Collaborative Innovation Center of Chemistry for Energy Materials, University of Science & Technology of China, Hefei, Anhui, 230029, China

KEYWORDS: Facet; Adsorption; in-situ DRIFTS; Hydroxyl group; Photocatalysis

ABSTRACT: The effective adsorption is of great importance to the photocatalytic degradation of volatile organic compounds. Herein, we succeeded in preparation of anatase TiO_2 with clean dominant {001} and {101} facets. By using in-situ diffuse reflectance infrared Fourier transform spectroscopy (DRIFTS) equipped with a homemade reaction system and a coupling gas-dosing system, we found that TiO_2 with dominant {001} facets exhibits higher toluene adsorption capacity than TiO_2 with dominant {101} facets, which may be attributed to the different number of unsaturated 5c-Ti capable of forming the main active adsorption sites (terminal Ti-OH

species). TiO_2 with dominant {001} facets shows a significantly high photocatalytic degradation performance, with its degradation rate being 6 times higher than that of dominant {101} facets. Combined with simulation results, it is suggested that the synergetic effects of the formation of specific active adsorption sites, the low adsorption energy for toluene and preservation of the free molecularly adsorbed water on the surface promote the degradation of gaseous toluene on the dominant {001} facets. This study exemplifies that the facet dependent adsorption of volatile organic compounds is one of the most important factor to engineer photocatalysts for air purification effectively.

1 Introduction

In the past decades, facet engineering and shape-fabrication of TiO_2 have attracted much research interest in environment and energy-related applications, such as photocatalytic splitting of water, photocatalytic degradation of pollutants and photocatalytic conversion of CO_2 into renewable hydrocarbon fuels.[1–5] For anatase TiO_2, conventional understanding indicates that the {001} facets are much more reactive than the thermodynamically more stable {101} facets due to their high surface energy and abundant unsaturated atoms.[6–9] It was then documented that the photocatalytic activity of different facets of anatase TiO_2 probably follow the order of the average surface energies, γ(110) 1.09 J m^{-2} > γ(001) 0.9 J m^{-2} > γ(100) 0.53 J m^{-2} > γ(101) 0.44 J m^{-2}.[10] As a result, an important breakthrough in preparation of anatase TiO_2 single crystals with exposed {001} facets were achieved by Lu and co-workers.[11] In addition, with regard to the facet dependent photocatalytic activity, the difference of preferential transport directions of photogenerated carriers is believed to be another factor.[12,13] It has been detected that the photogenerated electrons selectively migrate toward {101} facets, making {101} a suitable redox site, while photogenerated holes tend to migrate to {001} facets, making {001} an oxidation

site.[14] Therefore, more •OH radicals would be generated on {001} facets while more $\bullet O_2^-$ radicals might be formed on {101} facets. It is not surprising that the photocatalytic activity increases when increasing the percentage of {001} facets.[15,16] However, the photocatalytic activity decreases markedly when the percentage of the exposed {001} facets exceeds 70%.[17] It was realized that too less {101} facets hinder the separation of photogenerated carriers and achievement of high photocatalytic activity. Recently, first-principle calculations predicts the relative photooxidation ((100) > (101) > (001)) and photoreduction ((100) > (101) > (001)) activities, which rectify the conventional understandings.[18] Also in experiments, the researchers discovered the clean predominant {001} facets exhibit lower reactivity than {101} in photooxidation reactions for hydrogen evolution and degradation of organics in aqueous.[19,20] It appears that the detailed mechanism of facet dependent photocatalytic activity is still in its infant stage.

For photocatalytic degradation of volatile organic compounds (VOCs), not only above issues but also quantitative description of the adsorption behavior on different facets and in-depth understanding of adsorption energies on different facets should be further investigated. In terms of gaseous toluene, one typical VOC, it was speculated that the weak-bonding between the surface hydroxyl group and the aromatic ring of toluene adsorbed on TiO_2 was suggested to be the OH···π-electron-type interaction.[20–22] Therefore, the surface hydroxyl groups acting as active sites are crucial to toluene adsorption on TiO_2 surface.[23,24] In this paper, the dominant {001} and {101} facets of anatase TiO_2 were controllably synthesized. The facet dependent adsorption of toluene on TiO_2 was identified by using an in-situ DRIFTS apparatus equipped with a homemade reaction system and a coupling gas-dosing system. Combined with the theoretical simulation, the

relationship of facet structure, adsorption sites and photocatalytic degradation activity were proposed as well.

2 Experimental

2.1 Preparation of samples

TiO_2 with different dominant facets were prepared by a hydrothermal method.[17,25] For TiO_2 with exposed {001} facets, 50 mL $Ti(OC_4H_9)_4$ and 18 mL 40 wt.% HF as a shape directing agent were mixed under stirring to produce homogenous solution. The solution was transferred into a dry Teflon autoclave with a capacity of 100 mL, and then kept at 180 °C for 24 h. *Caution! HF is extremely corrosive and a contact poison, and it should be handled with extreme care.* After cooling down in atmosphere to room temperature, the white precipitate was separated by high-speed centrifugation, washed by the mixture of ethanol and deionized water (1:1) for several times to remove fluorine species, and then dried at 80 °C for 6 h. The as-synthesized sample was labeled as T001.

For TiO_2 with exposed {101} facets, a precursor was synthesized in advance. In a typical precursor preparation procedure, 0.6 g P25 (Degussa) was added into 70 mL 10 M KOH solution. After stirring mildly for several minutes, the mixture was put into a Teflon autoclave with a capacity of 100 mL and then kept at 200 °C for 48 h. After cooling down to room temperature, the precursor was separated by high-speed centrifugation, washed with deionized water until the pH reached about 7.0, and dried at 50 °C. The following hydrothermal reaction was carried out to obtain TiO_2 with exposed {101} facets. 0.05 g as-synthesized sample was mixed with 30 mL deionized water and then transferred into a 50 mL Teflon autoclave. The reaction was conducted at 200 °C for 3 h. Then the sample was separated, washed and dried in the same condition as the precursor synthesis procedure. Notably, it is unnecessary to add any

capping agents to form {101} facets because {101} facets are thermodynamically stable facets. The as-synthesized sample was labeled as T101.

2.2 Characterization

In the experiment, X-ray diffraction (XRD) patterns were carried out at room temperature to determine the crystalline structures of the samples by an X-ray diffractometer (TTR-III, Rigaku) with Cu-Kα radiation at a scan rate of 10°/min. The morphologies of the samples were characterized by a field emission scanning electron microscopy (FESEM, Sirion200, FEI) and transmission electron microscopy (TEM, JEM-2011). In order to observe the microstructures of exposed facets, high resolution transmission electron microscopy (HRTEM, JEM-2011) was used and the selected area electron diffraction (SAED) patterns were acquired simultaneously. The Raman spectra (inVia, Renishaw) were used to estimate the percentage of certain exposed facets. The wavelength of the excitation laser was 532 nm, and the exposure time was 10 s. The specific surface areas and X-ray photoelectron spectroscopy (XPS) study of the samples were listed in Supporting Information.

2.3 In-situ DRIFTS test

Toluene adsorption on the samples was investigated using in-situ DRIFTS equipped with a homemade reaction system and a coupling gas-dosing system (Figure S1). A Fourier transform infrared spectrometer (FTIR, IFS 66v/s, Bruker) was used to collect the infrared spectra in the range of 4000-800 cm^{-1} by averaging 40 scans with a resolution of 4 cm^{-1} at scanning velocity of 20 kHz. The reaction cell housing a sample cup was filled with photocatalysts. A dome with three windows covers the sample cup (Figure S2). Therein, one quartz window was used to observe the experiments, while the other two ZnSe windows were IR transparent. The purging gas of Ar, water vapor and reaction vapor of toluene were regulated by mass flow controllers

(Seven Star Electronics Co. Ltd) and then fed into the cell. The relative humidity level (R.H.) in the cell was fixed at 46% by a bypass with an electronic hygrometer. Details about the in-situ DRIFTS and the gas-dosing operation have been published elsewhere.[26–28] For further understanding the differences of adsorption property between the samples, the adsorption structure and energy of molecular toluene on different exposed surfaces were simulated by computational methods (Figure S3 and Table S1).[29,30]

2.4 Photocatalytic test

The photocatalytic activities were examined by measuring the degradation rate of gaseous toluene in a quartz reactor with the volume of 400 mL (Figure S4). In the experiments, 0.25g sample was first diffused into a certain amount of deionized water to obtain equivalent-volume impregnation, followed by coating on the inside of the reactor with an approximate area of 75 cm^2. The gaseous toluene was fed into the reactor by bubbling the compressed air through the saturators containing toluene with the aid of the same gas-dosing system in DRIFTS investigation. The relative humidity was regulated by another bypass. The initial concentration of toluene is 500 ppm, and the relative humidity level is R.H. 60%. Before the reaction, the sample was kept in dark for 30 min to reach the adsorption/desorption equilibrium on the photocatalyst surface. During the reaction, a Xe-arc lamp (PLS-SXE300/300UV, Beijing Perfectlight Technology Co. Ltd) with the light power of 215 mW at 365 nm and electric power of 300 W was used to irradiate the photocatalyst. At intervals, the concentration of toluene in the reactor was detected by a gas chromatography (GC1690, Hangzhou Kexiao Scientific Instruments Co. Ltd) equipped with a flame ionization detector (FID) and a chromatographic column (KX-112, Lanzhou Institute of Chemical Physics).

3 Results and discussion

Figure 1 shows the XRD patterns of the as-synthesized samples. The diffraction partterns of the two samples can be indexed to the pure anatase TiO_2 with tetragonal structure ($I4_1/amd$, JCPDS file No. 21-1272). The characteristic peaks at 25.28°, 36.95°, 37.8°, 38.58°, 48.05°, 53.89°, 55.96°, 62.69°, 68.76°, 70.31°, 75.03° and 76.02° are indexed to the facets of {101}, {103}, {004}, {112}, {200}, {105}, {211}, {204}, {116}, {220}, {215} and {301} of anatase TiO_2, respectively. All the prepared TiO_2 samples display a good crystallinity.

The morphology and microstructure of T001 are shown in Figure 2. SEM image (Figure 2a) and TEM image (Figure 2b) of the sample display a sheet-like shape of more than 100×100 nm^2 in size with a thickness around 10 nm. The SAED pattern in the inset of HRTEM image (Figure 2c) can be indexed to the diffraction spots of the [001] zone for the TiO_2 single crystalline, indicating that prepared T001 is exposed with the (001) facet. Also, the HRTEM image reveals more detail information of its atomic structure. The two vertical sets of lattice with the same fringe spacing of 0.19 nm are anatase (002) and (200) planes. Differently, T101 displays a morphology of bipyramid, as shown in Figure 3. It is apparent that the length of T101 sample is around 400 nm, and the side length of middle of the bipyramids is about 100 nm (Figure 3a and b). The existence of (101) facet in the SAED pattern (inset of Figure 3c) reflects that the sample exposes (101) facet. The HRTEM image (Figure 3c) provides the image of crystalline lattice of the dominant (101) facet. The three sets of lattice fringes with spacing of 0.48, 0.35, and 0.35 nm are associated with (002), (101), and (10−1) facets, respectively. The angle between the two sets of lattice corresponding to (002) facets and (101) facets is 68.3°. All of these characteristics strongly demonstrated the dominant (101) facet of as-synthesized T101 sample.

It is noticed in Figure 4 that T001 and T101 almost have the same peak positions in Raman spectra, namely 141 (E_g), 393 (B_{1g}), 515 (A_{1g}) and 634 (E_g) cm^{-1}. Among these peaks, the E_g

peak is mainly related to symmetric stretching vibration of O-Ti-O, the B_{1g} peak is related to symmetric bending vibration of O-Ti-O, and the A_{1g} peak is related to asymmetric bending vibration of O-Ti-O.[31] It can be seen that E_g peak of T001 is obviously weaker than that of T101. There are four kinds of bonding modes distributed on anatase TiO_2 {101} facets, including six-coordinated Ti atoms (6c-Ti), three-coordinated O atoms (3c-O), five-coordinated Ti atoms (5c-Ti) and two-coordinated O atoms (2c-O). As to {001} facets, only unsaturated 5c-Ti and 2c-O bonding modes are possible. Therefore, compared to {101} facets, the less symmetric stretching vibration modes of O-Ti-O can be observed on {001} facets. Furthermore, it can be deduced that more symmetric and asymmetric of O-Ti-O bending vibrates on the {001} surface, which was reflected by the enhanced intensity of the A_{1g} and B_{1g} peaks of T001 in Figure 4. Generally speaking, the percentage of {001} facets can be quantitatively determined by the intensity ratio of the E_g and A_{1g} peaks.[32] Based on this, the percentage of {001} facets of T001 was estimated about 67% (Table 1). The percentage of {101} facets of T101 is usually calculated indirectly by morphologic images. According to the SEM and TEM information in Figure 3, we can estimate that the percentage of {101} facets of T101 is 95% approximately.

~~For better comparing the adsorption of toluene on TiO_2 with different dominant facets, the specific surface areas of T001 and T101 are performed (Figure S5 and Table S2). In brief, the surface areas of the samples are similar, indicating that the difference in adsorption of toluene between the samples ***is not attributed*** to the surface areas in this study.~~ Figure 5 shows the DRIFTS spectra of T001 and T101 before toluene adsorption. As observed, the surfaces of both samples are abundant with hydroxyl groups since appearance of two broad bands at 3449 and 2991 cm^{-1}, and the narrow band at 1630 cm^{-1}, which can be assigned to O-H stretching mode ($\nu_{O\text{-}H}$) of the terminal Ti-OH, adsorbed water Ti-OH_2 species and H-O-H bending mode ($\delta_{H\text{-}O\text{-}H}$)

of free molecularly adsorbed water, respectively.[33–35] The relative intensity of the band at 3449 and 1630 cm^{-1} in the T001 is stronger than that in T101, while the intensity of the band at 2991 cm^{-1} in the T001 is obviously weaker than that in T101. This suggests that the hydroxyl groups tend to be formed as terminal Ti-OH on the {001} facets. Additionally, the preparation process of T001 preserved the free water to a large extent on the surface, while {101} facets favor the formation of adsorbed water Ti-OH_2 species. It is worth mentioning that no fluorine species was observed on the surface of T001 in DRIFTS spectra. The XPS results (Figure S6) also indicated that only a small amount of fluorine species appeared on T001. In other words, the fluorine species introduced in the synthetic process have been almost removed from the surface of as-synthesized T001, and hardly affect the adsorption of toluene on T001.

To grasp intuitively the gaseous toluene adsorption on different facets, in-situ DRIFTS spectra were collected on the as-synthesized T001 and T101 samples at room temperature. For T001 (Figure 6a), the new bands at 3084, 3059, 3042, 3023, 1490, 1450, 1432 and 1421 cm^{-1} appear after the introduction of toluene. The band at 3084 cm^{-1} can be assigned to C-H stretching vibrations of the aromatic ring. The bands at 3059, 3042 and 3023 cm^{-1} are assigned to asymmetric and symmetric C-H stretching vibrations of methyl group. The bands at 1490 cm^{-1} are assigned to in-plane skeletal vibration of the aromatic ring, and the bands at 1450, 1432 and 1421 cm^{-1} are ascribed to the asymmetric methyl bending vibration, respectively (details in Figure S7 and Table S3).[36,37] The intensity of these bands increases with increasing adsorption time and reaches a stable level after about 5 min. Similarly on the T101 surface (Figure 6b), the band at 3033 cm^{-1} corresponding to C-H stretching vibrations of the aromatic ring, the bands at 2929, 2917, 2909, 2853 and 2842 cm^{-1} corresponding to asymmetric and symmetric C-H stretching vibrations of methyl group, and the band at 1436 cm^{-1} corresponding to methyl

bending vibration also appear after introduction of toluene. It should be pointed out that the positions of these characteristic bands of adsorbed toluene on T101 are red-shifted slightly compared to that on T001, which may be attributed to the different Ti^{4+} adsorption sites on {001} and {101} facets for toluene adsorption.[38,39] Notably, the adsorption takes much longer for T101 to reach a stable level. For easy understanding, the integrated areas of the characteristic bands of C-H stretching vibrations of toluene on T001 and T101 facets as a function of adsorption time are shown in Figure 7. The toluene adsorption increases more rapidly on {001} facets with a relatively large adsorption quantity after reaching a stable level. The kinetics investigation indicated that the adsorption process on {001} facets is typically Langmuir-Hinshelwood model of first-order reaction, while the adsorption process on {101} facets is in agreement with two-step kinetic equation (Figure S8). The noticeable distinction of the adsorption capability probably results from the different surficial structures of certain exposed facets. As shown in Figure 8, the surface of (001) consists of coordinatively unsaturated 5c-Ti and 2c-O atoms, while (101) facet exposes 50% of unsaturated 5c-Ti and 2c-O atoms, and the remaining 50% are fully coordinated 6c-Ti and 3c-O atoms.[19,40] As known, Hydroxyl groups are generally formed by dissociative chemisorption of water molecules coming from atmospheric environment and preparation process to satisfy the coordination of the surface Ti^{4+} sites.[42–44] And the surface hydroxyl groups acting as active sites for toluene adsorption are crucial to toluene adsorption on TiO_2 surface because toluene is suggested to be adsorbed on TiO_2 via OH···π-electron-type interaction.[20,22,41] For T001, the unsaturated 5c-Ti atoms are probably favorable for formation of terminal Ti-OH species, which is reflected in Figure 5 and Figure 6 with high intensity of the band at 3449 cm^{-1}. Whereas for T101, it contains only 50% of 5c-Ti and the rest is 6c-Ti. Correspondingly, the sample adsorbs water Ti-OH_2 species resulting in the lower

intensity of terminal Ti-OH (3449 cm^{-1}) and the higher adsorbed water Ti-OH_2 species (2991 cm^{-1}), which is also obvious in Figure 5 and Figure 6. It can be concluded that terminal Ti-OH species promote the toluene adsorption. In other words, (001) facet exhibits a higher capacity of toluene adsorption than (101) facet due to its high exposed unsaturated 5c-Ti sites which are likely to adsorb water molecules to generate terminal Ti-OH. Furthermore, according to the theoretical simulation, the adsorption energy of molecular toluene on (001) facet with hydroxyl groups is −1.04 eV, while the value on (101) facet is −11.83 eV (Figure S3 and Table S1). It means that toluene adsorption on (101) facet need to overcome the higher energy barrier than that on (001) facet, resulting in the lower toluene adsorption on (101) facet. It should be pointed out that the surface area (Figure S5 and Table S2) of T101 (51.9 m^2/g) is even higher than that of T001 (37.9 m^2/g), which indicates that the higher capacity of toluene adsorption on T001 ***is not attributed*** to the difference in surface areas in this study.

In order to determine the relationship between the facet dependent adsorption and photocatalytic activity of TiO_2, the photocatalytic degradation of toluene on T001 and T101 was investigated (Figure 9). For comparison, the blank test for the self-photolysis of toluene without photocatalyst was also carried out. T001 exhibits dramatically higher degradation rate, about 6 times higher than T101 in the first 30 minutes. It almost completed decomposing the toluene in one hour. The possible reasons can be summarized as follows. Firstly, T001 offers fully unsaturated 5c-Ti atoms capable of forming terminal Ti-OH species, which in turn promotes the adsorption of toluene on the {001} facets via OH···π-electron-type interaction. Secondly, the abundant hydroxyl groups on T001 play an important role in toluene degradation because hydroxyl groups directly participate in the degradation process by trapping the charge carriers to produce very reactive •OH radicals.[45,46] In addition, it has been demonstrated that the

photogenerated holes tend to migrate to {001} facets, making the {001} an oxidation site to generate more •OH radicals.[42–44] Last but not least, the strong band at 1630 cm^{-1} in T001 sample (Figure 6a) suggests that the unsaturated 5c-Ti atoms benefit the preservation of the free molecularly adsorbed water on the surface of TiO_2. During the photocatalytic process, the molecularly water is probably continuing dissociated to form hydroxyls and further promote the degradation rate. These synergetic effects of surface adsorption are mainly responsible for the superiority of {001} facets in comparison with {101} facets in gaseous toluene degradation. Notably, in some literature[47], the surface fluorine species may enhance the photocatalytic activity for aqueous pollutants, while in some other literature[48], it did not improve the photocatalytic degradation of gaseous toluene. In this study, fluorine species were hardly observed from DRIFTS and did not affect the photocatalytic process.

4 Conclusions

Anatase TiO_2 nanoparticles exposed with dominant {001} and {101} facets were synthesized successfully via hydrothermal method. T001 contains about 67% of {001} facets and T101 contains about 95% of {101} facets. The toluene adsorption on different samples was investigated by in-situ DRIFTS and theoretical simulation. It was found that the different adsorption capacity of the two samples is mainly caused by the different distributions of 5c-Ti and 6c-Ti bonding modes on different facets. The terminal Ti-OH species tend to be formed on {001} facets, and provide the active sites for toluene adsorption. However, the {101} facets contain 50% coordinated 6c-Ti atoms which are favorable for the formation of $Ti\text{-}OH_2$ species. The outstanding photocatalytic degradation performance of TiO_2 with dominant {001} facets is mainly due to the high adsorption ability and the preservation of the free molecularly adsorbed

water, which can be continuing dissociated to form hydroxyls and further promote the degradation rate.

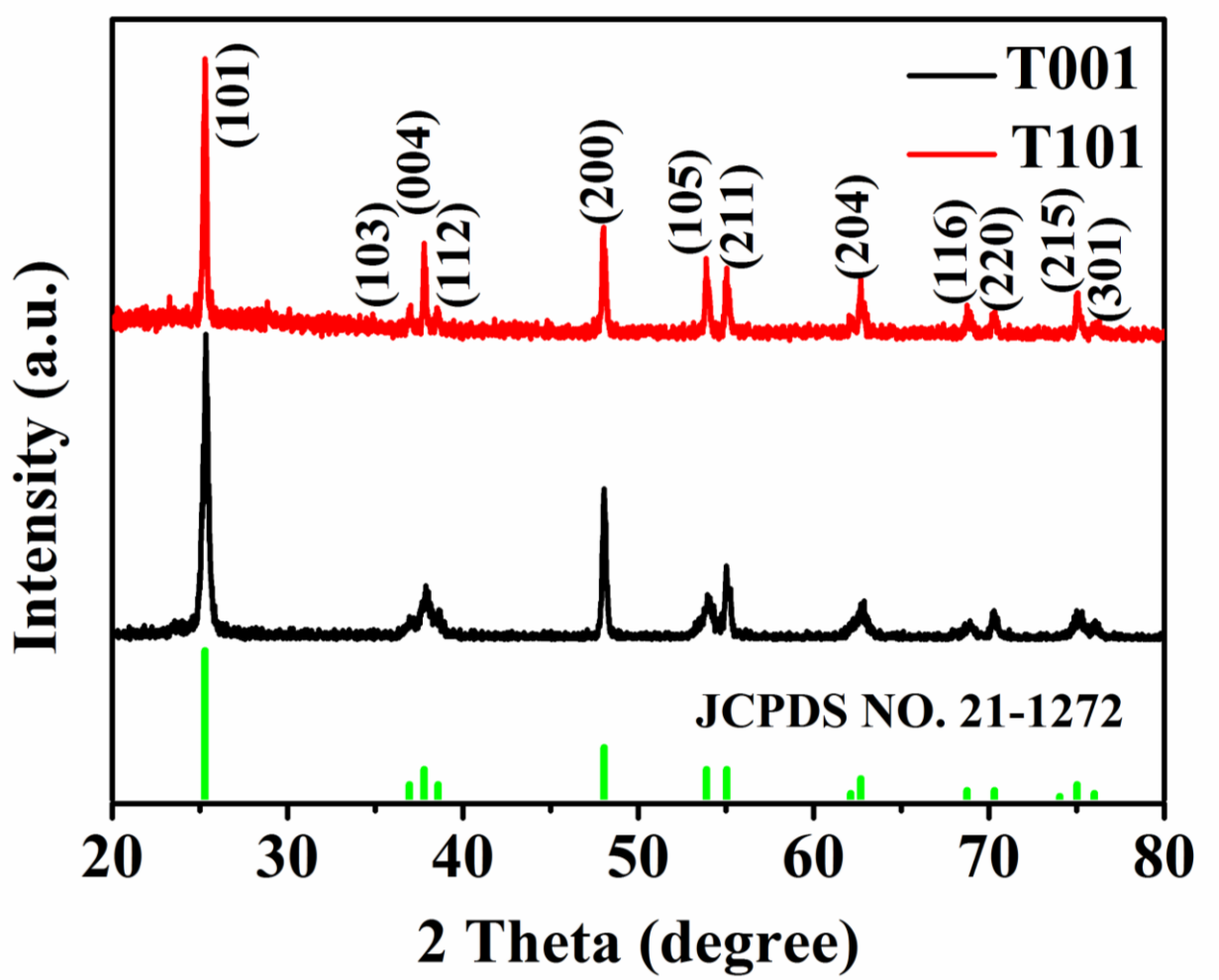

Figure 1. XRD patterns of T001 and T101.

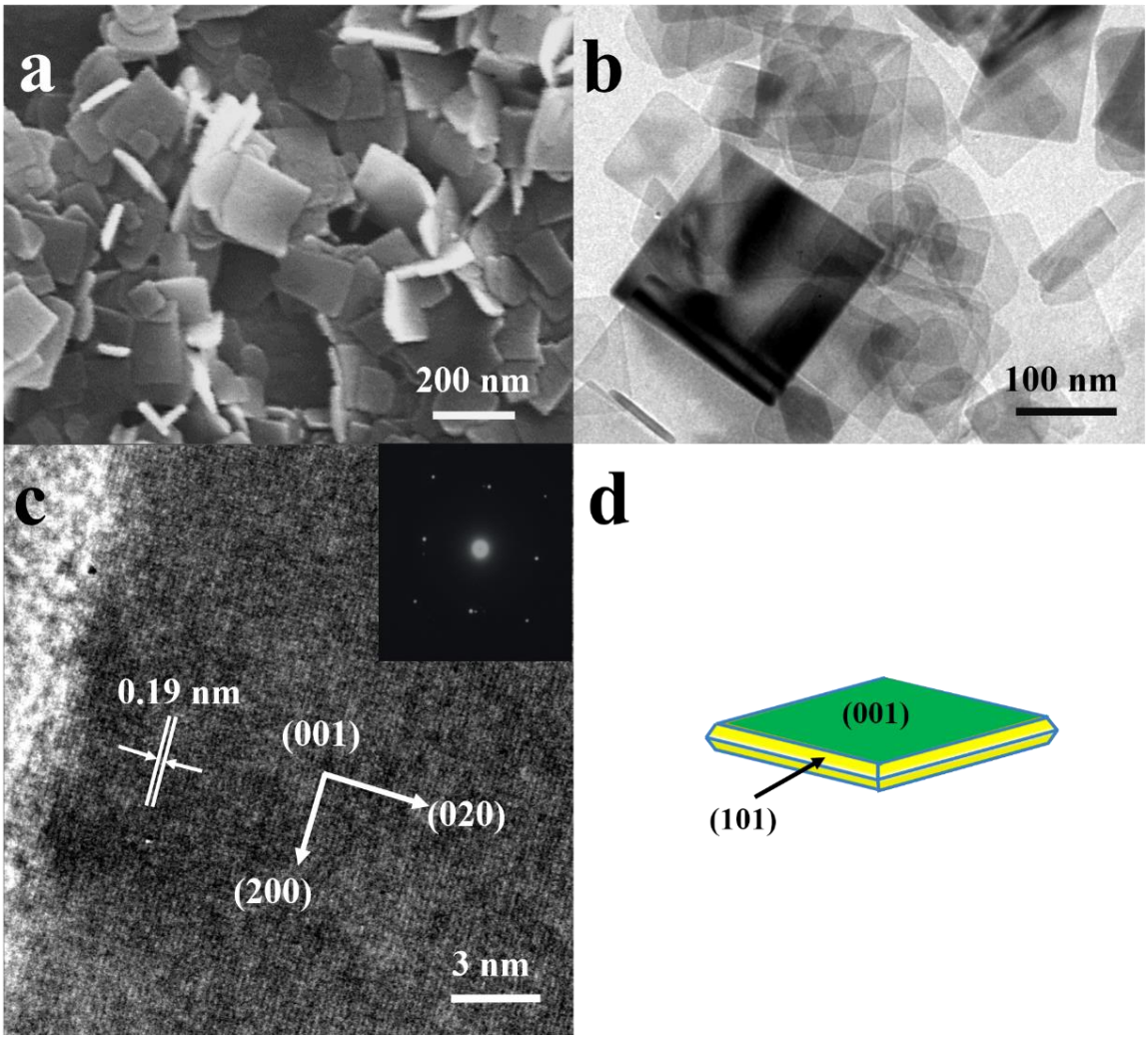

Figure 2. SEM image (a), TEM image (b), HRTEM image (c) and SAED pattern (inset of c), as well as the schematic illustration of T001 (d).

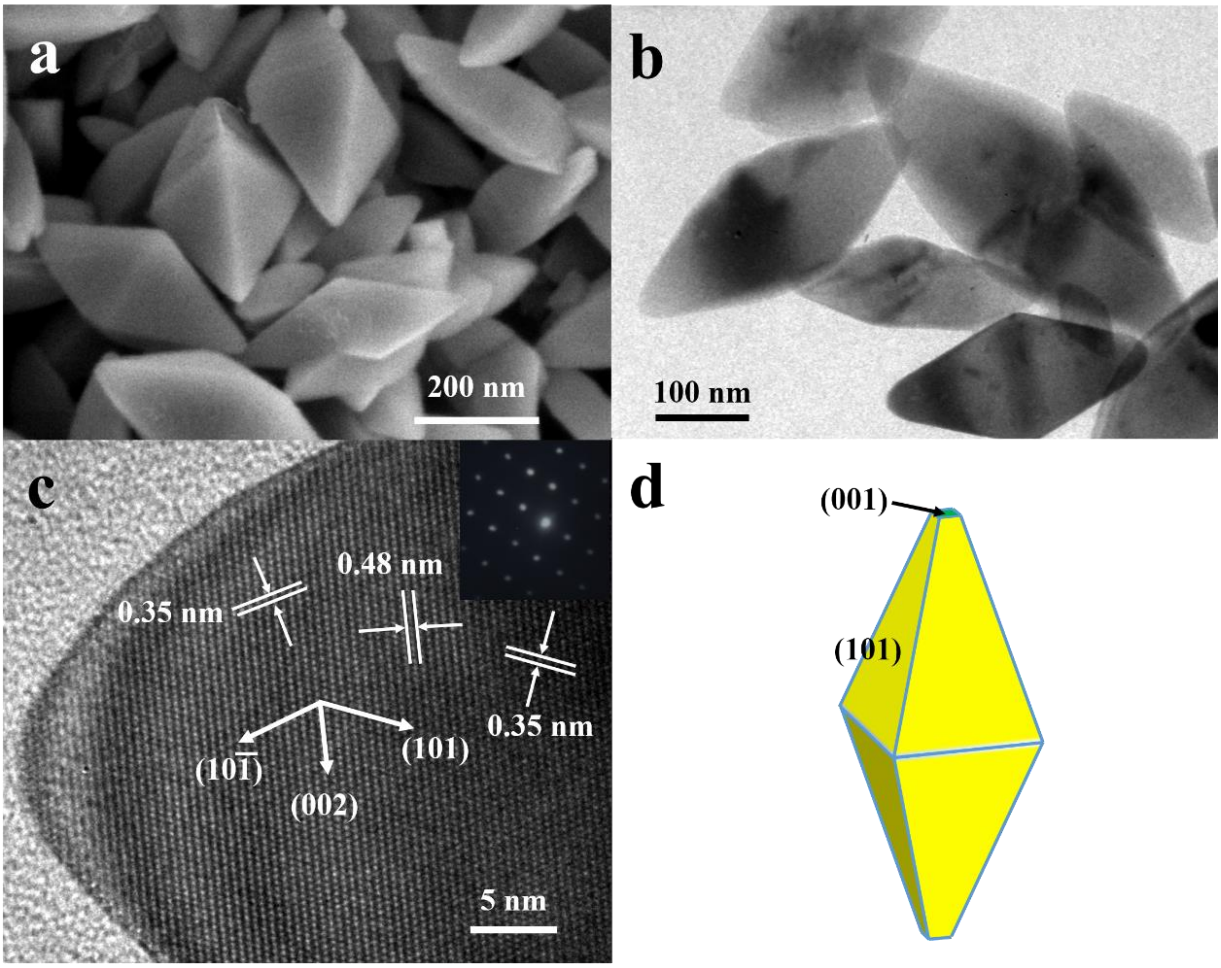

Figure 3. SEM image (a), TEM image (b), HRTEM image (c) and SEAD pattern (inset of c), as well as the schematic illustration of T101 (d).

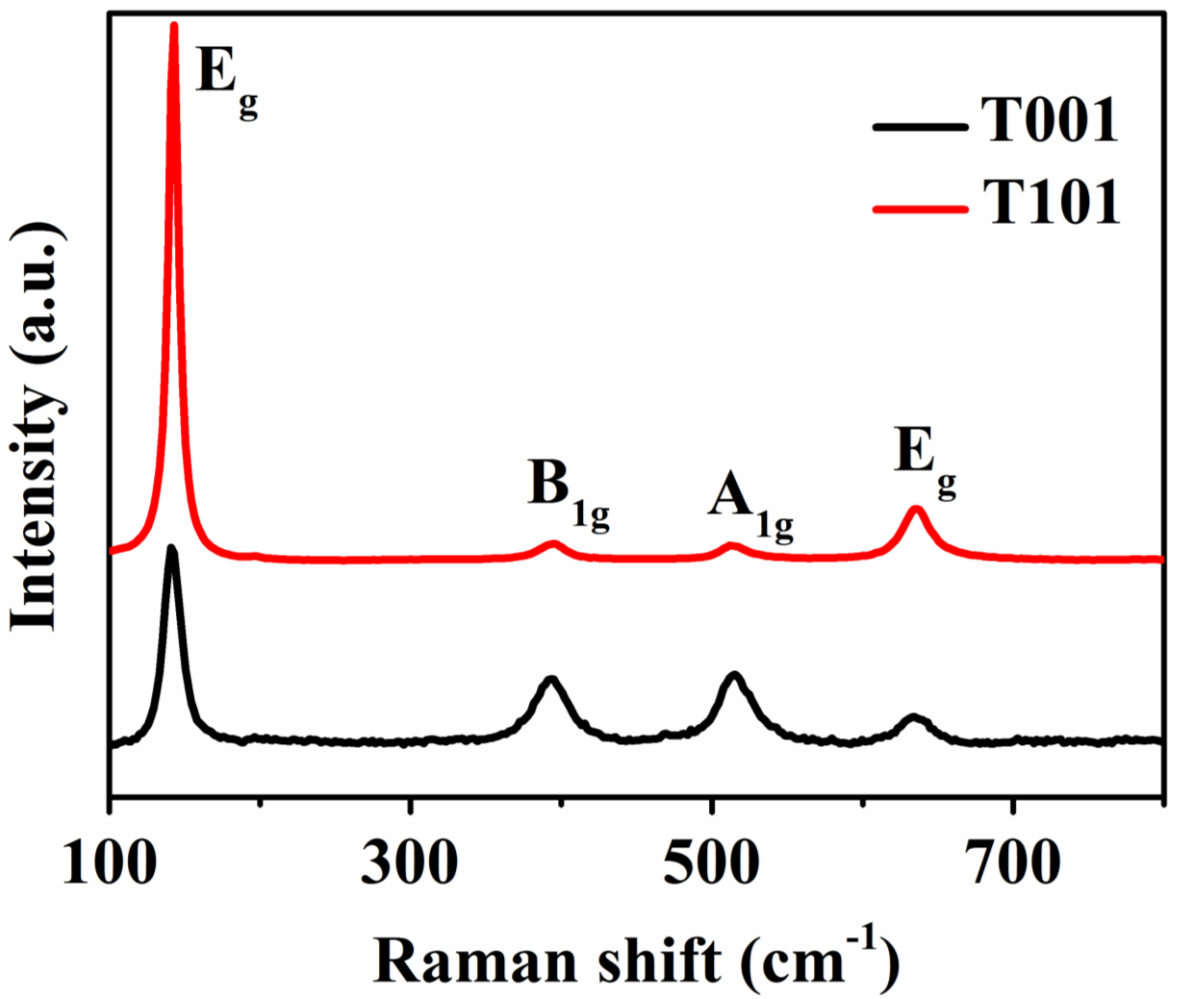

Figure 4. Raman spectra of T001 and T101.

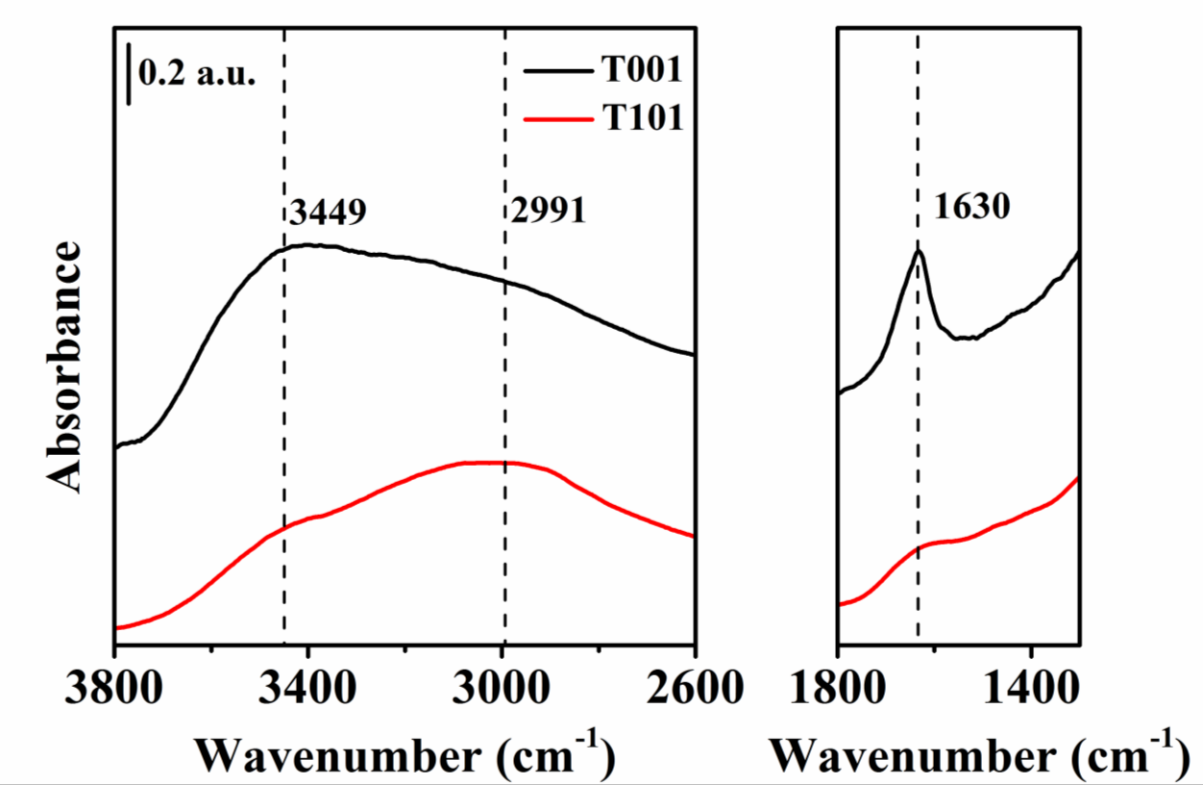

Figure 5. DRIFTS spectra of pure T001 and T101.

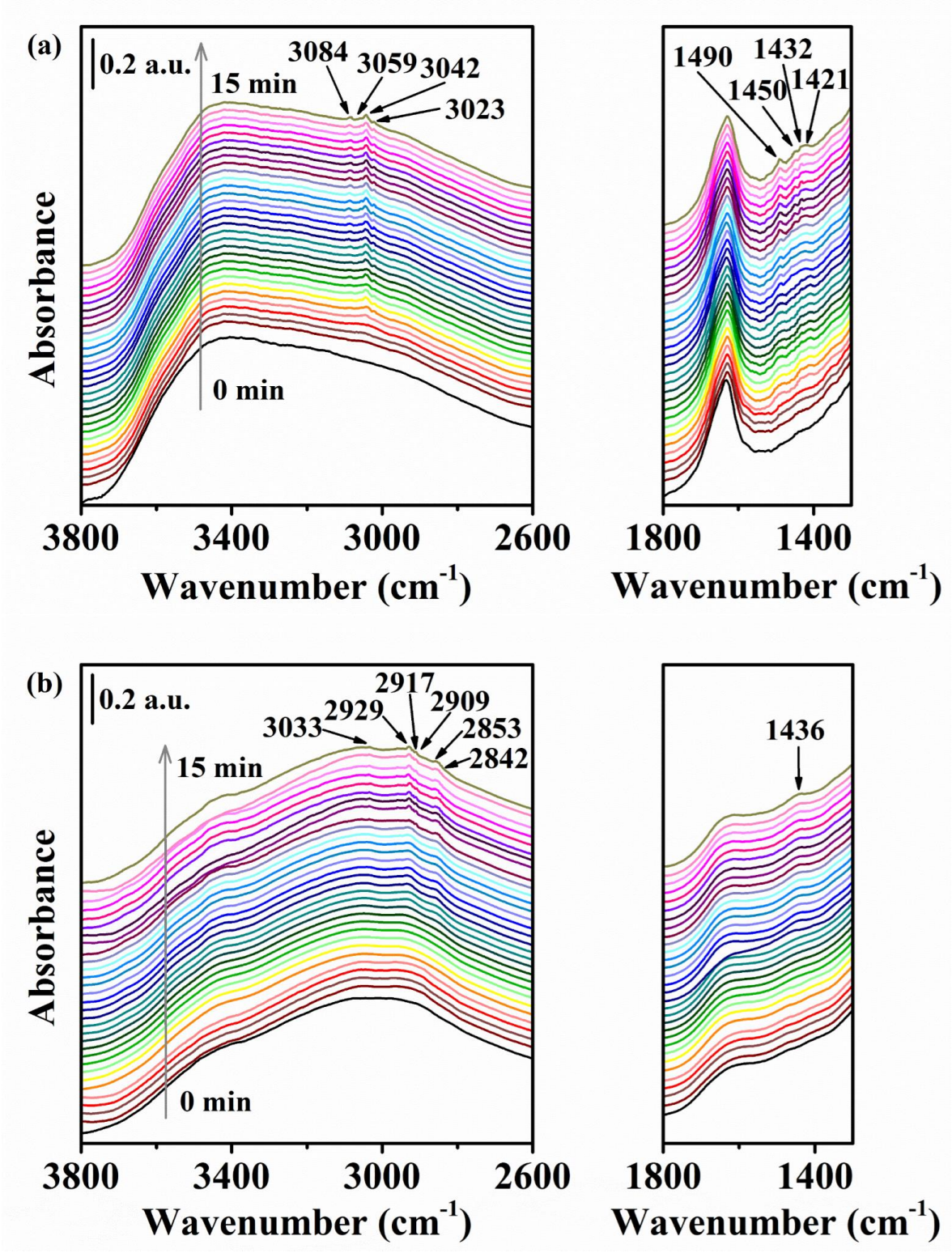

Figure 6. In-situ DRIFTS spectra of toluene adsorption on T001 (a) and T101 (b).

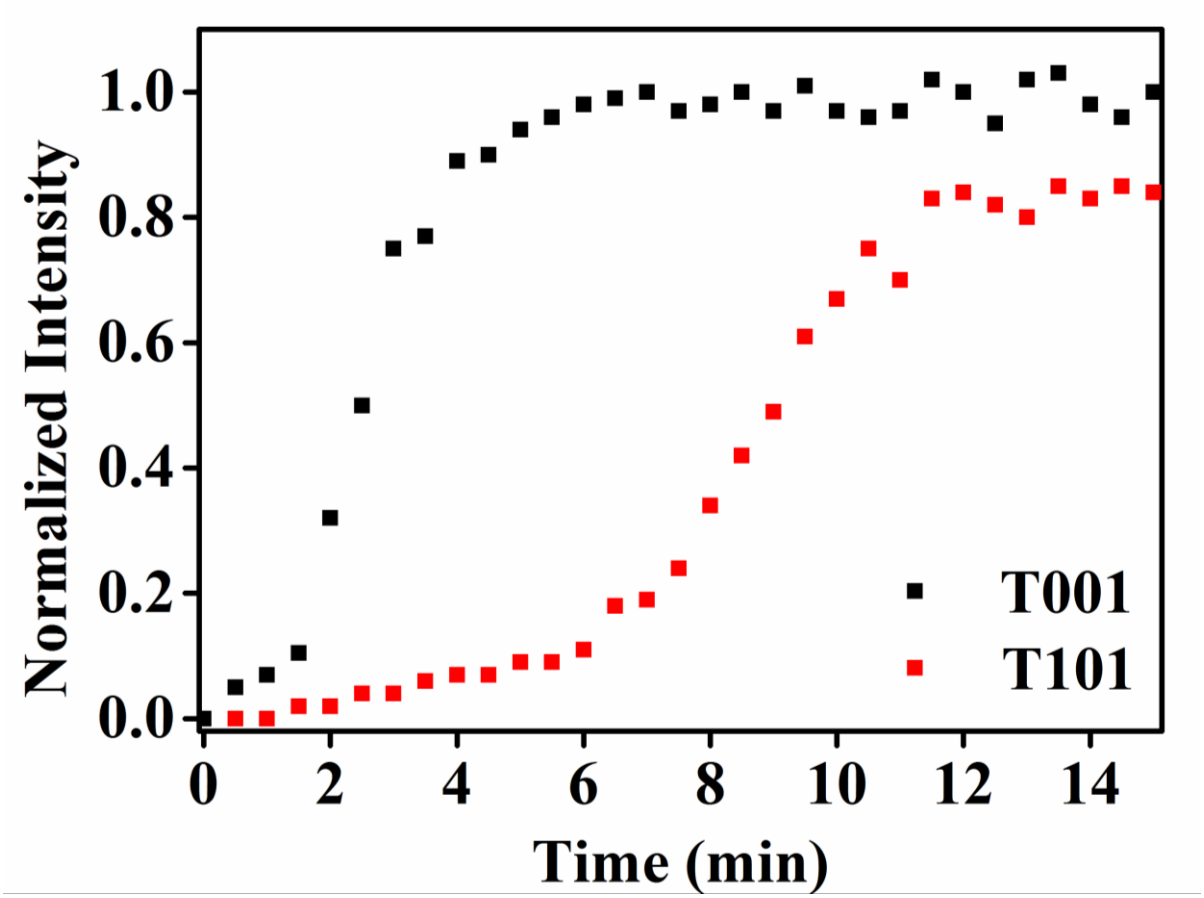

Figure 7. The integrated areas of the characteristic bands (C-H stretching vibrations of the aromatic ring) as the function of adsorption time of T001 and T101.

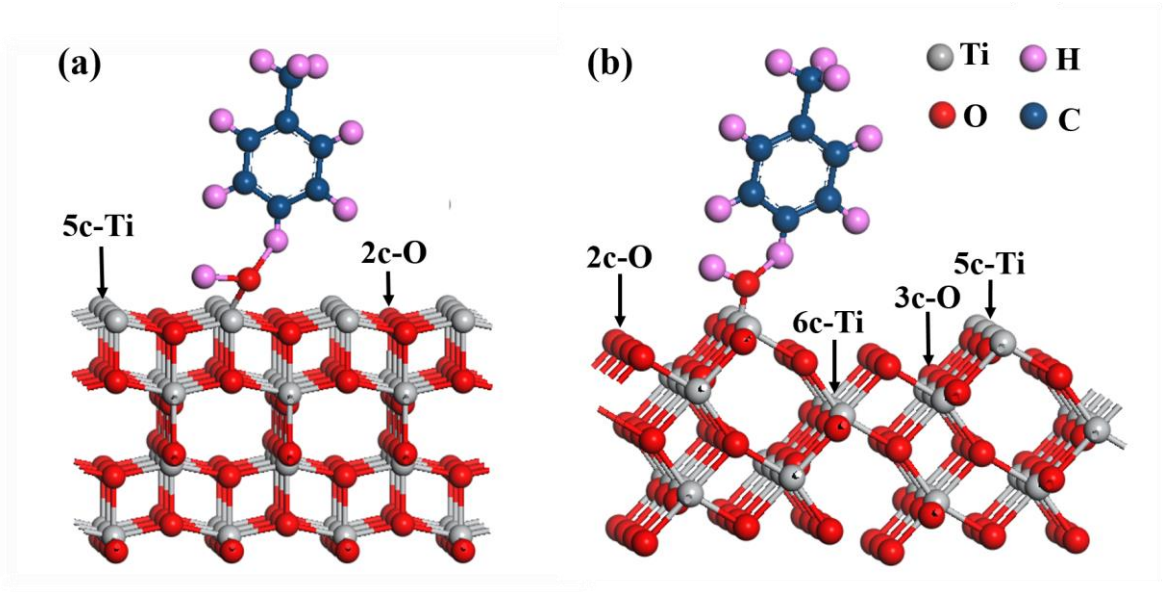

Figure 8. Optimized adsorption structures of toluene molecules adsorbed on (001) facet (a) and (101) facet (b) with hydroxyl groups.

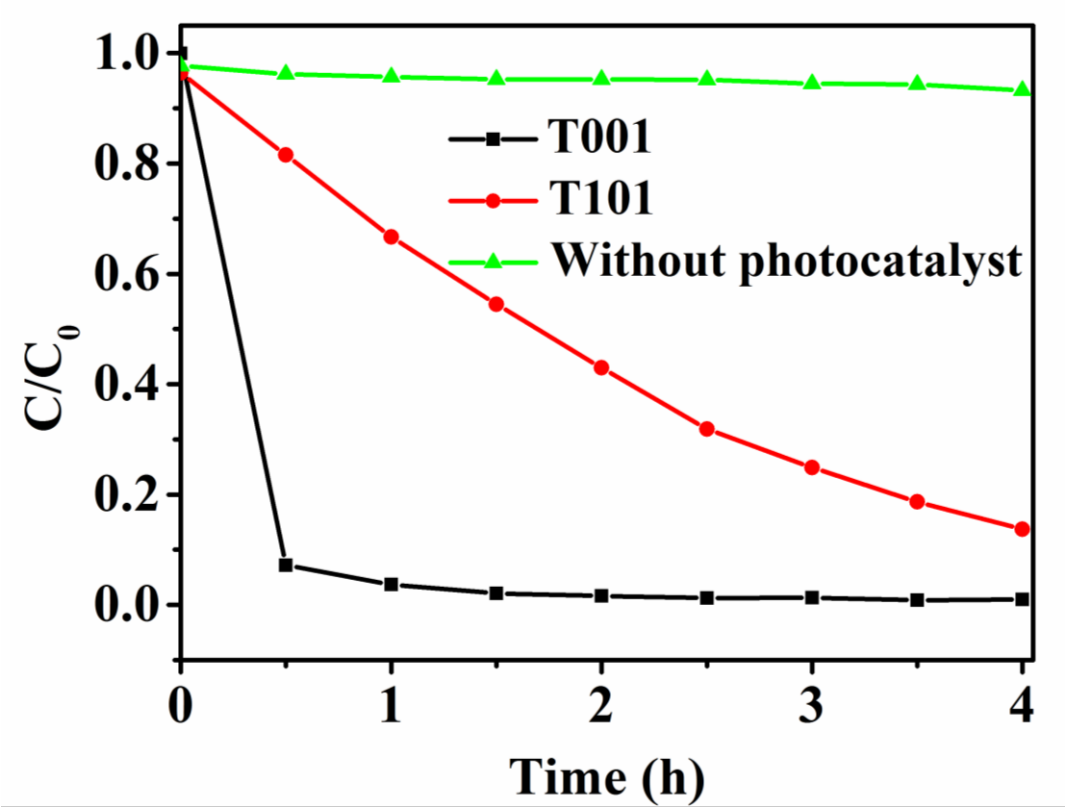

Figure 9. Photocatalytic degradation of gaseous toluene on T001 and T101.

Table 1. Intensity (Area) of Raman peaks and percentage of exposed {001} and {101} facets.

Samples	Peak area of E_g (141 cm^{-1})	Peak area of A_{1g} (515 cm^{-1})	Percentage of {001}	Percentage of {101}
T001	137361	92425	67%	33%
T101	859356	43216	5%	95%

ASSOCIATED CONTENT

Supporting Information

In-situ DRIFTS set-up for toluene adsorption, details of reaction cell, theoretical simulation, reactor for photocatalytic degradation, analysis of BET surface area and pore size distribution, analysis of XPS spectra, details of characteristic bands in DRIFTS spectra and kinetics of adsorption of toluene onto T001 and T101. This material is available free of charge via the Internet at http://pubs.acs.org.

AUTHOR INFORMATION

Corresponding Author

*Fax: (+86) 551-6514-1078. Tel: (+86) 551-6360-2031. E-mail: suns@ustc.edu.cn (S.Sun). E-mail: cgao@ustc.edu.cn (C.Gao)

Notes

The authors declare no competing financial interest.

ACKNOWLEDGMENT

This work was supported by National Basic Research Program of China (973 Program, 2012CB922004), National Nature Science Foundation of China (11205159, 11179034)~~,~~, Anhui Provincial Natural Science Foundation (1308085MB27, 1408085MB25). The authors thank Dr. Yuyin Wang and Tao Shao for assistance on the in-situ DRIFTS measurements.

ABBREVIATIONS

DRIFTS, diffuse reflectance infrared Fourier transform spectroscopy; XRD, X-ray diffraction; FESEM, field emission scanning electron microscopy; TEM, transmission electron microscopy; HRTEM, high resolution transmission electron microscopy; SAED, selected area electron diffraction.

REFERENCES

(1) Xu, H.; Ouyang, S.; Li, P.; Kako, T.; Ye, J. High-Active Anatase TiO_2 Nanosheets Exposed with 95% {100} Facets Toward Efficient H_2 Evolution and CO_2 Photoreduction. *ACS Appl. Mater. interfaces* **2013**, *5*, 1348–1354.

(2) Wang, D.; Kanhere, P.; Li, M.; Tay, Q.; Tang, Y.; Huang, Y.; Sum, T. C.; Mathews, N.; Sritharan, T.; Chen, Z. Improving Photocatalytic H_2 Evolution of TiO_2 via Formation of {001} - {010} Quasi-Heterojunctions. *J. Phys. Chem. C* **2013**, *117*, 22894–22902.

(3) Wu, Q.; Wu, Z.; Li, Y.; Gao, H.; Piao, L.; Zhang, T.; Du, L. Controllable Synthesis and Photocatalytic Activity of Anatase TiO_2 Single Crystals with Exposed {110} Facets *Chin. J. Cata.* **2012**, *33*, 1743–1753.

(4) Jiao, W.; Wang, L.; Liu, G.; Lu, G. Q.; Cheng, H.-M. Hollow Anatase TiO_2 Single Crystals and Mesocrystals with Dominant {101} Facets for Improved Photocatalysis Activity and Tuned Reaction Preference. *ACS Catal.* **2012**, *2*, 1854–1859.

(5) Zhou, L.; Chen, J.; Ji, C.; Zhou, L.; O'Brien, P. A Facile Solid Phase Reaction to Prepare TiO_2 Mesocrystals with Exposed {001} Facets and High Photocatalytic Activity. *CrystEngComm* **2013**, *15*, 5012–5015.

(6) Liu, M.; Piao, L.; Zhao, L.; Ju, S.; Yan, Z.; He, T.; Zhou, C.; Wang, W. Anatase TiO_2 Single Crystals with Exposed {001} and {110} Facets: Facile Synthesis and Enhanced Photocatalysis. *Chem. Commun.* **2010**, *46*, 1664–1666.

(7) Yang, H. G.; Liu, G.; Qiao, S. Z.; Sun, C. H.; Jin, Y. G.; Smith, S. C.; Zou, J.; Cheng, H. M.; Lu, G. Q. Solvothermal Synthesis and Photoreactivity of Anatase TiO_2 Nanosheets with Dominant {001} Facets. *J. Am. Chem. Soc.* **2009**, *131*~~(11)~~, 4078–4083.

(8) Sofianou, M. V.; Trapalis, C.; Psycharis, V.; Boukos, N.; Vaimakis, T.; Yu, J.; Wang, W. Study of TiO_2 Anatase Nano and Microstructures with Dominant {001} Facets for NO Oxidation. *Environ. Sci. Pollut. Res.* **2012**, *19*, 3719–3726.

(9) Xu, H.; Reunchan, P.; Ouyang, S.; Tong, H.; Umezawa, N.; Kako, T.; Ye, J. Anatase TiO_2 Single Crystals Exposed with High-Reactive {111} Facets Toward Efficient H_2 Evolution. *Chem. Mater.* **2013**, *25*, 405–411.

(10) Lazzeri, M.; Vittadini, A.; Selloni, A. Structure and Energetics of Stoichiometric TiO_2 Anatase Surfaces. *Phys. Rev. B* **2001**, *63*, 155409.

(11) Yang, H. G.; Sun, C. H.; Qiao, S. Z.; Zou, J.; Liu, G.; Smith, S. C.; Cheng, H. M.; Lu, G. Q. Anatase TiO_2 Single Crystals with a Large Percentage of Reactive Facets. *Nature* **2008**, *453*, 638–641.

(12) Tachikawa, T.; Yamashita, S.; Majima, T. Evidence for Crystal-Face-Dependent TiO_2 Photocatalysis from Single-Molecule Imaging and Kinetic Analysis. *J. Am. Chem. Soc.* **2011**, *133*, 7197–7204.

(13) Murakami, N.; Kurihara, Y.; Tsubota, T.; Ohno, T. Shape-Controlled Anatase Titanium(IV) Oxide Particles Prepared by Hydrothermal Treatment of Peroxo Titanic Acid in the Presence of Polyvinyl Alcohol. *J. Phys. Chem. C* **2009**, *113*, 3062–3069.

(14) Roy, N.; Sohn, Y.; Pradhan, D. Synergy of Low-Energy {101} and High-Energy {001} TiO_2 Crystal Facets for Enhanced Photocatalysis. *ACS nano* **2013**, *7* (3), 2532–2540.

(15) Maitani, M. M.; Tanaka, K.; Mochizuki, D.; Wada, Y. Enhancement of Photoexcited Charge Transfer by {001} Facet-Dominating TiO_2 Nanoparticles. *J. Phys. Chem. Lett.* **2011**, *2*, 2655–2659.

(16) Fang, W. Q.; Gong, X.; Yang, H. G. On the Unusual Properties of Anatase TiO_2 Exposed by Highly Reactive Facets. *J. Phys. Chem. Lett.* **2011**, *2*, 725–734.

(17) Liu, C.; Han, X.; Xie, S.; Kuang, Q.; Wang, X.; Jin, M.; Xie, Z.; Zheng, L. Enhancing the Photocatalytic Activity of Anatase TiO_2 by Improving the Specific Facet-Induced Spontaneous Separation of Photogenerated Electrons and Holes. *Chem. Asian J.* **2013**, *8*, 282–289.

(18) Ma, X.; Dai, Y.; Guo, M.; Huang, B. Relative Photooxidation and Photoreduction Activities of the {100}, {101}, and {001} Surfaces of Anatase TiO_2. *Langmuir* **2013**, *29*, 13647–13654.

(19) Pan, J.; Liu, G.; Lu, G. Q.; Cheng, H. M. On the True Photoreactivity Order of {001}, {010}, and {101} Facets of Anatase TiO_2 Crystals. *Angew. Chem. Int. Ed.* **2011**, *50*, 2133–2137.

(20) Augugliaro, V.; Coluccia, S.; Loddo, V.; Marchese, L.; Martra, G.; Palmisano, L.; Schiavello, M. Photocatalytic Oxidation of Gaseous Toluene on Anatase TiO_2 Catalyst: Mechanistic Aspects and FT-IR Investigation. *Appl. Catal., B* **1999**, *20*, 15–27.

(21) Lin, H.; Long, J.; Gu, Q.; Zhang, W.; Ruan, R.; Li, Z.; Wang, X. In Situ IR Study of Surface Hydroxyl Species of Dehydrated TiO_2: towards Understanding Pivotal Surface Processes of TiO_2 Photocatalytic Oxidation of Toluene. *Phy. Chem. Chem. Phys.* **2012**, *14*, 9468–9474.

(22) Nagao, M.; Suda, Y. Adsorption of Benzene, Toluene, and Chlorobenzene on Titanium Dioxide. *Langmuir* **1989**, *5*, 42–47.

(23) Okamoto, K.; Yamamoto, Y.; Tanaka, H.; Tanaka, M.; Itaya, A. Heterogeneous Photocatalytic Decomposition of Phenol over TiO_2 Powder. *Bull. Chem. Soc. Jpn.* **1985**, *58*, 2015–2022.

(24) Luo, Y.; Tai, W. S.; Seo, H. O.; Kim, K.-D.; Kim, M. J.; Dey, N. K.; Kim, Y. D.; Choi, K. H.; Lim, D. C. Adsorption and Photocatalytic Decomposition of Toluene on TiO_2 Surfaces. *Catal. Lett.* **2010**, *138*, 76–81.

(25) Xiang, Q.; Lv, K.; Yu, J. Pivotal Role of Fluorine in Enhanced Photocatalytic Activity of Anatase TiO_2 Nanosheets with Dominant (001) Facets for the Photocatalytic Degradation of Acetone in Air. *Appl. Catal., B* **2010**, *96*, 557–564.

(26) Zhang, F.; Zhu, X.; Ding, J.; Qi, Z.; Wang, M.; Sun, S.; Bao, J.; Gao, C. Mechanism Study of Photocatalytic Degradation of Gaseous Toluene on TiO_2 with Weak-Bond Adsorption Analysis Using In Situ Far Infrared Spectroscopy. *Catal. Lett.* **2014**, *144*, 995–1000.

(27) Sun, S.; Ding, J.; Bao, J.; Gao, C.; Qi, Z.; Li, C. Photocatalytic Oxidation of Gaseous Formaldehyde on TiO_2: An In Situ DRIFTS Study. *Catal. Lett.* **2010**, *137*, 239–246.

(28) Sun, S.; Zhang, F.; Qi Z.; Ding, J.; Bao, J.; Gao, C. Rapid Discovery of a Photocatalyst for Air Purification by High-Throughput Screening. *ChemCatChem* **2014**, *6* ~~(9)~~, 2535–2539.

(29) Dong, H.; Zhang, L.; Zhou, X. Theoretical Investigation on RuO_2 Nanoclusters Adsorbed on TiO_2 Rutile (110) and Anatase (101) Surfaces. *Theor. Chem. Acc.* **2014**, *133*, 1496.

(30) Zhao, W.; Tian, F. H.; Wang, X.; Zhao, L.; Wang, Y.; Fu, A.; Yuan, S.; Chu, T.; Xia, L.; Yu, J. C.; Duan, Y. Removal of Nitric Oxide by the Highly Reactive Anatase TiO_2 (001) Surface: A Density Functional Theory Study. *J. Colloid Interface Sci.* **2014**, *430*, 18–23.

(31) Su, W.; Zhang, J.; Feng, Z.; Chen, T.; Ying, P.; Li, C. Surface Phases of TiO_2 Nanoparticles Studied by UV Raman Spectroscopy and FT-IR Spectroscopy. *J. Phys. Chem. C* **2008**, *112*, 7710–7716.

(32) Tian, F.; Zhang, Y.; Zhang, J.; Pan, C. Raman Spectroscopy: A New Approach to Measure the Percentage of Anatase TiO_2 Exposed (001) Facets. *J. Phys. Chem. C* **2012**, *116*, 7515.

(33) Maira, A. J.; Coronado, J. M.; Augugliaro, V.; Yeung, K. L.; Conesa, J. C.; Soria, J. Fourier Transform Infrared Study of the Performance of Nanostructured TiO_2 Particles for the Photocatalytic Oxidation of Gaseous Toluene. *J. Catal.* **2001**, *202*, 413–420.

(34) Connor, P. A.; Dobson, K. D.; McQuillan, A. J. Infrared Spectroscopy of the TiO_2/Aqueous Solution Interface. *Langmuir* **1999**, *15*, 2402–2408.

(35) Murcia, J. J.; Hidalgo, M. C.; Navío, J. A.; Araña, J.; Doña-Rodríguez, J. M. In Situ FT-IR Study of the Adsorption and Photocatalytic Oxidation of Ethanol over Sulfated and Metallized TiO_2. *Appl. Catal., B*, **2013**, *142*, 205–213.

(36) Besselmann, S.; Löffler, E.; Muhler, M. On the Role of Monomeric Vanadyl Species in Toluene Adsorption and Oxidation on V_2O_5/TiO_2 Catalysts: a Raman and In Situ DRIFTS Study. *J. Mol. Catal. A: Chem.* **2000**, *162*, 401–411.

(37) Sun, S.; Ding, J.; Bao, J.; Gao, C.; Qi, Z.; Yang, X.; He, B.; Li, C. Photocatalytic Degradation of Gaseous Toluene on Fe-TiO_2 under Visible Light Irradiation: A Study on the Structure, Activity and Deactivation Mechanism. *Appl. Surf. Sci.* **2012**, *258*, 5031–5037.

(38) Gong, X.; Selloni A.; Vittadini A. Density Functional Theory Study of Formic Acid Adsorption on Anatase TiO_2(001): Geometries, Energetics, and Effects of Coverage, Hydration, and Reconstruction. *J. Phys. Chem. B* **2006**, *110*, 2804–2811.

(39) Lin, J. S.; Chou, W. ; Lu, S.; Jang, G.; Tseng, B.; L,i Y. Density Functional Study of the Interfacial Electron Transfer Pathway for Monolayer-Adsorbed InN on the TiO_2 Anatase (101) Surface. *J. Phys. Chem. B* **2006**, *110*, 23460–23466.

(40) Vittadini, A.; Selloni, A.; Rotzinger, F. P.; Grätzel, M. Structure and Energetics of Water Adsorbed at TiO_2 Anatase (101) and (001) Surfaces. *Phys. Rev. Lett.* **1998**, *81* ~~(14)~~, 2954–2957.

(41) Bianchi, C. L.; Gatto, S., Pirola, C., Naldoni, A., Di Michele, A., Cerrato, G.; Crocellà, V.; Capucci, V. Photocatalytic Degradation of Acetone, Acetaldehyde and Toluene in Gas-phase: Comparison between Nano and Micro-sized TiO_2. *Appl. Catal., B* **2014**, *146*, 123–130.

(42) Gong, X.; Selloni, A. Reactivity of Anatase TiO_2 Nanoparticles: The Role of the Minority (001) Surface. *J. Phys. Chem. B* **2005***, 109,* 19560–19562.

(43) Blomquist, J.; Walle, L. E.; Uvdal, P.; Borg, A.; Sandell, A. Water Dissociation on Single Crystalline Anatase TiO_2(001) Studied by Photoelectron Spectroscopy. *J. Phys. Chem. C* **2008**, *112*, 16616–16621.

(44) Sumita, M.; Hu, C.; Tateyama, Y. Interface Water on TiO_2 Anatase (101) and (001) Surfaces: First-Principles Study with TiO_2 Slabs Dipped in Bulk Water. *J. Phys. Chem. C* **2010**, *114*, 18529–18537.

(45) Yu, J.; Xiang, Q.; Ran, J.; Mann, S. One-step Hydrothermal Fabrication and Photocatalytic Activity of Surface-fluorinated TiO_2 Hollow Microspheres and Tabular Anatase Single Micro-crystals with High-energy Facets. *CrystEngComm* **2010**, *12* ~~(3)~~, 872–879.

(46) Liu, G.; Sun, C.; Yang, H. G.; Smith, S. C.; Wang, L.; Lu, G. Q.; Cheng, H. M. Nanosized Anatase TiO_2 Single Crystals for Enhanced Photocatalytic Activity. *Chem. Commun. (Camb)* **2010**, *46* ~~(5)~~, 755–757.

(47) Umadevi, M.; Parimaladevi, R.; Sangari, M. Synthesis, characterization and photocatalytic activity of fluorine doped TiO_2 nanoflakes synthesized using solid state reaction method. *Spectrochim. Acta, Part A* **2014**, *120*, 365–369.

(48) Lewandowski, M.; Ollis, D. F. Halide acid pretreatments of photocatalysts for oxidation of aromatic air contaminants: rate enhancement, rate inhibition, and a thermodynamic rationale. *J. Catal.* **2003**, *217*, 38–46.

TOC Graphic

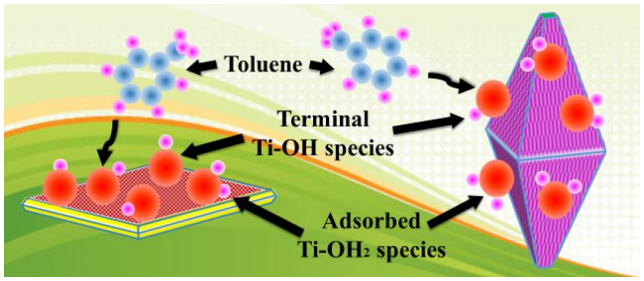

In-situ DRIFTS provide direct evidence for facet dependent adsorption of gaseous toluene on TiO_2, which can be explained by the different structures and numbers of active adsorption sites. The work exemplifies that the facet engineering is an effective way to enhance the photocatalytic performance for air purification.